Elaboration of spherical particles of PMMA/ZnO through macroporous polymer networks

Humberto Monreal[1,2] ✉, *Carolina Zubia*[1], *Diana Sagarnaga*[1], *Teresa Perez*[1], *Carlos Martìnez*[3], *Jose Chacon*[2]

[1]*Departamento de Ciencia de Materiales, Universidad Autónoma de Chihuahua (UACH), Av. Universidad S/n, CP 31000 Chihuahua, Chih., Mexico*
[2]*Centro de Investigación en Materiales Avanzados, S.C. (CIMAV), Av. Miguel de Cervantes 120, Complejo Industrial Chihuahua, Chihuahua CP 31136, Chih, Mexico*
[3]*Instituto de Ingeniería y Tecnología, U.A.C.J. Avenida del Charro # 610 Norte Cd. Juárez, Chihuahua, Mexico*
✉ *E-mail: hmonreal@uach.mx*

Published in Micro & Nano Letters; Received on 22nd February 2018; Revised on 19th July 2018; Accepted on 15th August 2018

In this study, it is explained how spherical particles of poly(methyl methacrylate) (PMMA)/ZnO were synthesised in the presence of a polymer matrix of galactopyranose for their control growth. The objective of this research is to show the development of particles using the sol–gel method and the participation of a polysaccharide network. This method can increase the formation of stable spherical particles due to the hydrogen bonds junctions present in the walls of the polysaccharide network. The results of the formed tablets immersed in simulated body fluid indicate that there is no evidence of corrosion in the presence of PMMA/ZnO nanoparticles. The maximum roughness average (R_{max}) and roughness value (R_a) were 0.41 and 1.27 nm, respectively. The absorbance values showed significant changes when 10% polysaccharide concentration was used both in the presence and absence of the PMMA/ZnO nanoparticles. The particles were characterised by scanning electron microscopy, atomic force microscopy, powder X-ray diffraction (PXRD), X-ray elemental mapping, ultraviolet–visible spectrophotometry, and energy dispersive X-ray spectroscopy. The PXRD analysis shows the crystalline and amorphous phases of the composite at 400°C. The size range of the synthesised particles was between 30 and 100 μm.

1. Introduction: Poly(methyl methacrylate) (PMMA) is a very versatile polymer that has many applications in the fields of medicine, dentistry, and industry due to its physical and chemical characteristics [1]. In the same way, several methods have been developed for the synthesis of various structures such as micro- and nanoparticles, vehicles for the release of drugs at the cellular level, among others [2, 3]. One of the applications that has drawn great attention is the elaboration of ocular lenses and prosthetic materials for dentistry and medicine, which have been mixed with other types of materials such as zinc oxide to form bone matrix [4]. There are also other PMMA/ZnO joints to synthesise grafts [5]. In the study of biocompatibility of these materials, studies on the HeLa linkage can be highlighted, in which the biosafety effectiveness of the PMMA/ZnO nanoparticles is demonstrated [6]. The other uses of PMMA/ZnO particles in the electrical field include the manufacture of composites for the dielectric permittivity study through the casting technique [7]. In the same way, the mechanical and electrical properties of the PMMA/ZnO nanocomposites have been explored using the Unsaturated Polyester (UPE) polymer in solution, finding a significant improvement in their properties [8]. Another application of PMMA/ZnO spherical particles is to study their optical properties for the modification of the refractive index of the measured precipitation [9]. Similarly, a method was proposed for evaluating the response of ethanol's overheating to synthesise temperature sensors using PMMA [10]. Various techniques have been developed for the synthesis of PMMA/ZnO particles such as in situ emulsion polymerisation for evaluating their electrical conductivity [11]. In addition, the functions of PMMA/ZnO nanocomposites have been used in the field of solar cells to acquire a greater thermal control through microwave heating by using the reflux method [12]. From these studies arose a need to look for different alternatives of synthesis such as the casting method, the sol–gel technique, polymerisation experiments, synthesis at the ZnO nanoscale in PMMA and its characterisation [13, 14].

2. Materials and methods: For the synthesis of PMMA/ZnO particles, a solution of 300 ml of ethanol and 70 ml of acetic acid was used to which 20 g of PMMA $(C_5O_2H_8)n$ and 10 g of ZnO were added. Subsequently, this solution was added to a 10% aqueous solution with 0.3 g of galactopyranose polymer, which was previously heated in a Corning PC-351 hot plate magnetic stirrer to a temperature of 30°C for 30 s to form a gel. In this way, once the polymer matrix is formed, the growth control of the PMMA/ZnO particles is achieved in an organised way within the matrix pores. Once the gel containing the particles was formed, it was placed in a 1.5 ml tube and centrifuged at 12,000 rpm in an Eppendorf 5424 microcentrifuge for 5 min at room temperature to form a tablet, then it was washed for 3 min with deionised water to clean the gel residues and was dried for 5 min and placed in a flask furnace Felisa 340 at 400°C for 1 h. The resulting powders were subsequently stored until they were used for the test in a simulated body fluid (SBF).

2.1. Preparation of SBF: The SBF was prepared by mixing the following laboratory reagents: sodium bicarbonate, sodium chloride, buffer tris(hydroxymethyl)aminomethane, pH 7.25, potassium chloride, calcium chloride, dibasic potassium phosphate, hydrogen chloride, and sodium sulphate into deionised water, according to the Kokubo method [15].

2.2. Preparation of PMMA/ZnO particles to test in SBF: To conduct the test of the PMMA/ZnO particles in a SBF solution, a 10% solution of 1 ml of acetone was prepared to which 1 g of PMMA/ZnO particles was added for a period of 15 min in a Cole Parmer 8892 ultrasonic cleaner, subsequently the particles were compacted forming tablets at 4000 psi with dimensions of 1 cm

doi: 10.1049/mnl.2018.5333

in diameter and 3 mm thickness in a hydraulic press machine (Monarch). Once the tablets were formed, they were immersed in SBF at 36.5°C for 4 weeks in a Neslab Exacal Bath Circulator EX 200DD. Afterwards, the tablets were washed several times and dried at room temperature for a day to be analysed by scanning electron microscopy (SEM; JEOL 444) and atomic force microscopy (AFM) (Nanosurf); the crystalline phase of powders was identified by powder X-ray diffraction (PXRD) using a CuK (α) source at 0.1542 nm in a Phillips X'PERT X-Ray diffractometer. The chemical elements were characterised by energy dispersive X-ray spectroscopy (EDX) and X-ray elemental mapping.

2.3. Preparation of samples for absorbance: Firstly, a 10% solution was prepared with 0.3 g of polysaccharide in 50 ml tubes with deionised water in the absence of PMMA/ZnO. A second 10% solution was prepared with 0.3 g of polysaccharide to which the PMMA/ZnO composite was added in 50 ml tubes with deionised water. Subsequently, the absorbance of both solutions was measured by an ultraviolet–visible (UV–Vis) spectrophotometer using quartz cuvettes ranging from 190 to 1100 nm.

3. Results and discussion: The compounds were morphologically characterised by SEM. Fig. 1*a* shows an image of particles of 30–100 µm diameters. In Fig. 1*b*, one can see the composite tablets once they were compacted to perform the analysis corresponding to the test in the SBF. Fig. 2 shows an SEM image of a PMMA/ZnO in the absence of the polysaccharide network and Fig. 3 shows an aggregate of the PMMA/ZnO spherical particles in the presence of the polysaccharide network. In these images, it is clearly shown that the importance of the polymer matrix participation in the creation of spherical morphology; besides the fact that there is an electrostatic interaction in the union of the PMMA molecules and zinc oxide due to the ionic packaging in which there is a greater presence of cations when the polysaccharide network is near, which would greatly exceed

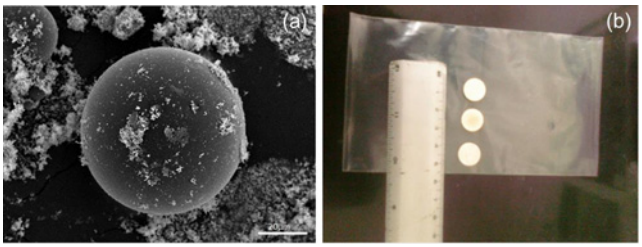

Fig. 1 *Compounds of PMMA/ZnO particles*
a PMMA/ZnO particles,
b PMMA/ZnO tablets with the applied method SEM

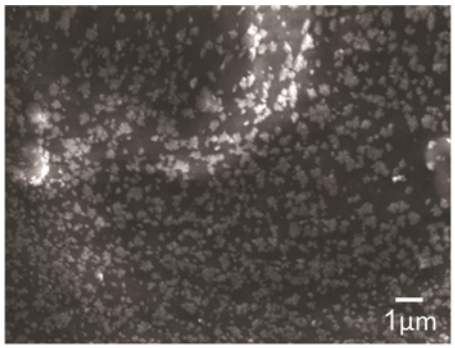

Fig. 2 *PMMA/ZnO in the absence of the polysaccharide network with the applied method SEM*

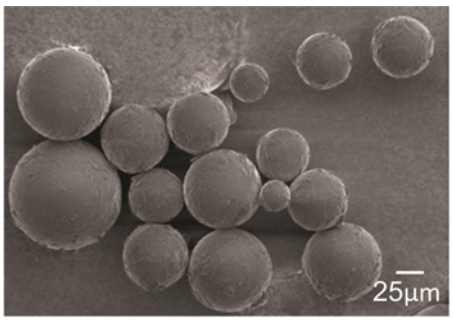

Fig. 3 *PMMA/ZnO particles formed in the presence of the polysaccharide network with the applied method SEM*

the concentration of anions; these cations can occupy the gaps that remain between the layers. In this manner, the formation of particles is a process in which the polysaccharide array plays a very important role due to the fact that its fibres start the process of gelation, therefore, the sol solution is slowly converted to gel and in this way the particles maintain a controlled growth by means of the polysaccharide network, avoiding loss of energy when the PMMA and ZnO precursors are interact.

Similarly, the morphology is controlled by the interfacial energies that include the free energy present in the polymer network, PMMA/ZnO nanoparticles, volume and interface's free energies, achieving a balance to organise the system and to make way for the development of microstructures without decreasing the total free energy of the whole mechanism.

In Fig. 4*a*, AFM shows the topography of the surface of the PMMA/ZnO tablets after being exposed to the SBF. In Fig. 4*b*, one can see (in 3D) the valleys and ridges that make up the composites and Fig. 5 shows a profile that corresponds to the behaviour of the roughness during the testing of the SBF. The results show an average of maximum roughness (R_{max}) of 0.41 nm, which corresponds to the difference of the maximum height of the peak and

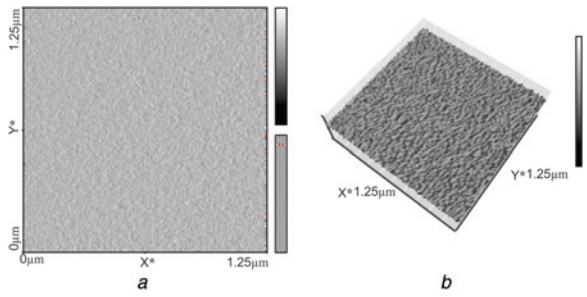

Fig. 4 *Images of PMMA/ZnO in SBF*
a AFM images
b 3D images

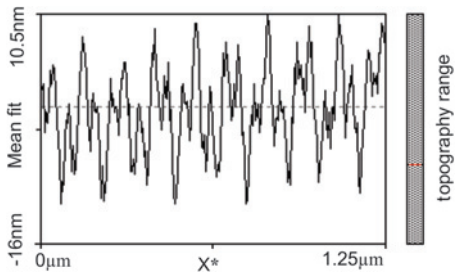

Fig. 5 *Roughness profile. Maximum roughness (R_{max}) and average roughness (R_a)*

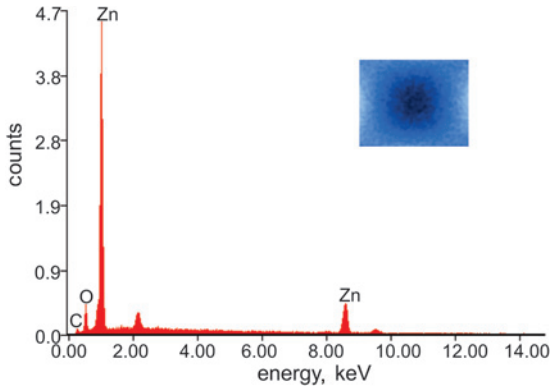

Fig. 6 *EDX spectrum of PMMA/ZnO particles*

the depth of the valley and a value of average roughness (R_a) of 1.27 nm that corresponds to the distances of roughness along the medium line, which were not altered during the time of tests. Similarly, the results in the SBF do not show evidence of corrosion, since the particles contain ZnO which can act against the corrosive effects of the medium inhibiting the processes of enolisation.

The EDX analysis shows the elemental composition of the sample where zinc oxide, oxygen, and carbon can be identified, Fig. 6.

The distribution of the chemical elements can be observed by means of X-ray elemental mapping, Fig. 7.

Table 1 shows the percentage of carbon, oxygen and zinc content in the samples. Considering the chemical composition, the zinc content is low due probably to the carbon oxides formation.

Fig. 8 shows the characteristics of the diffraction peaks of the PMMA/ZnO composite, the different peaks correspond to 32°, (100), 34° (002), 36° (101), 57°, (110), 48° (102), 63° (103), 68° (112), 69° (201),72° (004), 76° (202), 81° (104), 89° (203), 92° (210), 95° (211), 98° (114), 102° (212), 104° (105), 107° (2014), 110° (300), 116° (213), 121° (302), 125° (006), 133° (205), 136° (106), and 138° (214), respectively. The corresponding peaks show a crystalline phase of hexagonal Wurtzite ZnO. Besides, the graph shows a bulge at ∼13 (2θ), which corresponds

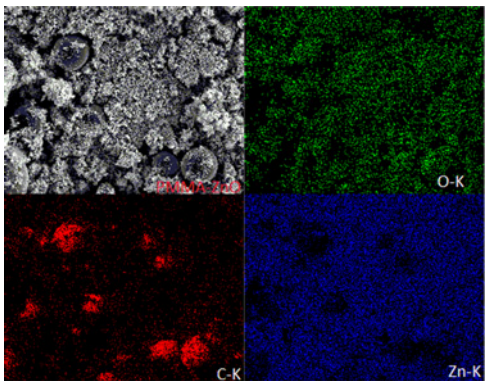

Fig. 7 *Oxygen, carbon, and zinc by X-ray elemental mapping*

Table 1 Chemical composition of PMMA/ZnO particles

Element	Wt%	At%
C K	92.66	95.75
O K	04.87	03.78
Zn K	02.47	00.47

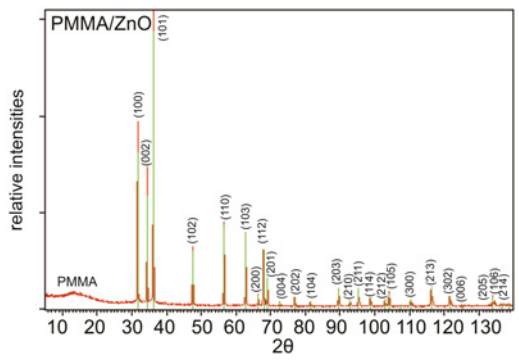

Fig. 8 *PXRD obtained for the sample of PMMA/ZnO particle*

to the PMMA in its amorphous phase. Similar results have been found in works carried out by Uthirakumar *et al.* [16].

The absorbance of the polymer at a 10% concentration containing the PMMA/ZnO composite was measured by UV–Vis spectroscopy. Fig. 9 shows an absorbance that begins with an increase at 280 nm and decreases to ∼390 nm for the ZnO. Additionally, the ZnO absorbance is observed with an increase of 410 and 500 nm then a decrease of 420 and 510 nm, respectively, is observed. In Fig. 9, a peak between 430 and 490 nm is observed, which corresponds to the PMMA. These differences may be due to the effects of loads developed on the surface of the polymer network with the increase in the intensity of absorption affecting principally the OH and O_2 groups. The results obtained are similar to those found by different authors [17–20]. Our hypothesis of the behaviour in the absorbance is that morphology probably plays an important role to activate the absorbance due to the participation of intramolecular hydrogen bonding of the polymer network thus achieving a better stability in the energy bands. In addition, the uses of different polymers during particle formation and preparation techniques promote different absorption fields that depend on the method of fabrication, size, and temperature.

These results clearly show the differences between all the system's components and the importance of the polysaccharide network participation in the intermolecular junction of the PMMA/ZnO nanoparticles for the spherical particles formation.

The proposed method contributed towards the synthesis' technical facility and the morphology's control of spherical particles using a polysaccharide network in comparison with other methods found in the literature since these methods can turn out be very laborious and expensive. Similarly, this method presents an advantage over the industrial scale production, because, for each 0.3 g of polymer matrix produced, ∼500 g of particles is obtained within 1 h and 20 min and using a minimal amount of equipment and chemical reagents. It is important to emphasise that there is a really good particle size (measurement) distribution, as well as the roughness values of the tablet complexes in the

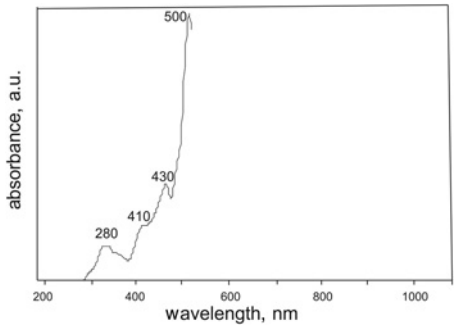

Fig. 9 *Absorbance of PMMA/ZnO composite*

doi: 10.1049/mnl.2018.5333

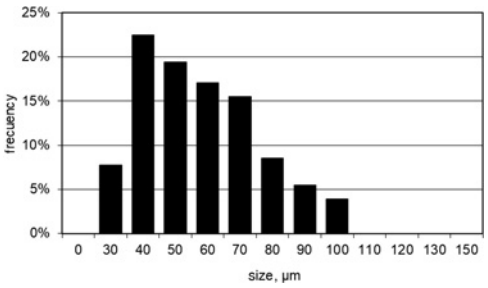

Fig. 10 *Particle size distribution of PMMA/ZnO particles*

presence of PMMA/ZnO particles. The size distribution of spherical particles can be influenced by the gap formation of the polymer network and by the walls flexibility during the polymerisation processes. Fig. 10 shows the differences in the size, which is in the range of 30–100 µm.

In this context, it is important to note that these results are consistent with other techniques carried out in various works reported in the literature in the formation of particles [20, 21]. In the same way, we have reported PMMA particles of 5 nm size by using the proposed solvent evaporation technique [22].

4. Conclusion: The galactopyranose polymer network is an efficient alternative to generate spherical particles. The efficiency of this system can be increased by means of its concentration. The obtained results of the PMMA/ZnO composites do not show evidence of corrosion, this aspect is very important when galactopyranose polymers are used. The roughness values found to allow a correct operation within the atomic scale for the use of particles at micro- and nanoscale. The absorbance of the polymer network sample and the sample containing PMMA/ZnO exhibits a remarkable difference in the range of 190–1100 nm due to the presence of the PMMA/ZnO nanoparticles. The methodology used activates the particles encapsulation through ionic interactions present in the system and exhibits excellent physicochemical properties. In addition, the interactions carried out in the molecular interfaces modify the superficial adsorption capacity reducing in this way the chemical corrosion processes in SBF. The possibility of synthesising microstructured materials using the polymeric network allows a control over the size, shape, and capacity of molecular self-assembly of inorganic compounds.

5. Acknowledgments: In this research, we would like to thank Wilber Antunez and C. Saenz for their technical assistance.

6 References

[1] Hench L.L.: 'Bioceramics: from concept to clinic', *J. Am. Ceram. Soc.*, 1991, **74**, (7), pp. 1487–1510
[2] Kumar R., Prakash K., Cheang P., *ET AL.*: 'Temperature driven morphological changes of chemically precipitated hydroxyapatite nanoparticles', *Langmuir*, 2004, **20**, (13), pp. 5196–5200
[3] Peng Z., Feng C., Luo Y., *ET AL.*: 'Self-assembled natural rubber/multi-walled carbon nanotube composites using latex compounding techniques', *Carbon*, 2010, **48**, (15), pp. 4497–4503
[4] Kondraske G.V.: 'Measurement tools and processes in rehabilitation engineering', in Bronzino J. D. (ed.) 'The Biomedical Engineering Handbook', vol. 2, pp. 145-141–145-116 (CRC Press, Boca Raton, FL, 2000)
[5] Hong R.Y., Qian J.Z., Cao J.X.: 'Synthesis and characterization of PMMA grafted ZnO', *Powder Technol.*, 2006, **163**, (3), pp. 160–168
[6] Hou L., Rusen Y., Min Y., *ET AL.*: 'Cellular level biocompatibility and biosafety of ZnO nanowires', *Phys. Chem. C*, 2008, **112**, (51), pp. 20114–20117
[7] Yadav G., Roy V., Kumar N.: 'Current-voltage and capacitive behavior of zinc oxide: poly(methyl methacrylate) composite films', *Int. J. Inn. Sci.*, 2016, **3**, (8), pp. 2348–7968
[8] Fadhil K., Farhan Z., Al R., *ET AL.*: 'Electrical and mechanical properties of ZnO/(UPE-PMMA) blend nanocomposites', *Int. J. Compos. Mater.*, 2017, **7**, (2), pp. 46–50
[9] Mustafa M., Demir K., Koynov Ü., *ET AL.*: 'Optical properties of composites of PMMA and surface-modified zincite nanoparticles', *Macromolecules*, 2007, **40**, (4), pp. 1089–1100
[10] Haibao L., Wei M., Huang X., *ET AL.*: 'Heating/ethanol-response of poly methyl methacrylate (PMMA) with gradient pre-deformation and potential temperature sensor and anti-counterfeit applications', *Smart Mater. Struct.*, 2014, **23**, (6), pp. 1–14
[11] Maneesh K., Poddar S., Sharma V., *ET AL.*: 'Investigations in two-step ultrasonic synthesis of PMMA/ZnO nanocomposites by in situ emulsion polymerization', *Polymer*, 2016, **99**, (2), pp. 453–469
[12] Soumya S., Peer M., Lucy P., *ET AL.*: 'Near IR reflectance characteristics of PMMA/ZnO nanocomposites for solar thermal control interface films', *Sol. Energy Mater. Sol. Cells*, 2014, **125**, (1), pp. 102–112
[13] Majid K., Mingming C., Chengsha W.T., *ET AL.*: 'Synthesis at the nanoscale of ZnO into poly(methyl methacrylate) and its characterization', *Appl. Phys. A*, 2014, **117**, (3), pp. 1085–1093
[14] Peng L., Zhixing S.: 'Preparation and characterization of PMMA/ZnO nanocomposites via in-situ polymerization method', *J. Macromol. Sci. B*, 2006, **45**, (1), pp. 131–138
[15] Kokubo T., Kushitani H., Sakka S., *ET AL.*: 'Solutions able to reproduce in vivo surface-structure changes in bioactive glass-ceramic A-W3', *J. Biomed. Mater. Res.*, 1990, **24**, (6), pp. 721–734
[16] Periyayya U., Youn L., Eun S., *ET AL.*: 'ZnO nanoballs synthesized from a single molecular precursor via non-hydrolytic solution route without assistance of base, surfactant, and template', *Phys. Lett. A*, 2006, **359**, (3), pp. 223–226
[17] Junlin G., Xiaofei Z., Xia T., *ET AL.*: 'Preparation and characterization of PS-PMMA/ZnO nanocomposite films with novel properties of high transparency and UV-shielding capacity', *J. Appl. Polym. Sci.*, 2010, **118**, (3), pp. 1507–1512
[18] Nahida J.: 'Spectrophotometric analysis for the UV-irradiated (PMMA)', *Int. J. Basic Appl. Sci.*, 2012, **12**, (02), pp. 58–67
[19] Koorosh F., Masoud N., Ghasem R., *ET AL.*: 'Dopamine determination with a biosensor based on catalase and modified carbon paste electrode with zinc oxide nanoparticles', *Int. J. Electrochem. Sci.*, 2012, **7**, (10), pp. 9892–9908
[20] Hamid R., Ghorbai F., Parsa M., *ET AL.*: 'Synthesis of ZnO nanoparticles by precipitation method', *Orient. J. Chem.*, 2015, **31**, (2), pp. 1219–1221
[21] Mitsugi I., Yusuke T., Takashi T., *ET AL.*: 'Beads mill-assisted synthesis of poly methyl methacrylate (PMMA)-TiO_2 nanoparticle composites', *Ind. Eng. Chem. Res.*, 2008, **47**, (8), pp. 2597–2604
[22] Zhanhu G., Laurence L., Henry V., *ET AL.*: 'Synthesis of poly(methyl methacrylate) stabilized colloidal zero-valence metallic nanoparticles', *J. Mater Chem.*, 2006, **16**, (18), pp. 1772–1777